

Observation of a knee in the p+He energy spectrum below 1 PeV by measuring particle densities very close to the EAS core with the ARGO-YBJ experiment

A. D'Amone, I. De Mitri*, L. Perrone, A. Surdo (for the ARGO-YBJ collaboration)

*Dipartimento di Matematica e Fisica "E. De Giorgi" - Università del Salento
and Istituto Nazionale di Fisica Nucleare (INFN) - Sezione di Lecce*

Via per Arnesano, I-73100, Lecce, Italy

E-mail: ivan.demitri@le.infn.it

The CR spectrum has been studied by the ARGO-YBJ experiment in a wide energy range ($10^{12} \rightarrow 10^{16}$ eV). This study is particularly interesting because not only it allows a better understanding of the so called knee of the energy spectrum and of its origin, but also provides a powerful cross-check among very different experimental techniques. The unique detector features (full coverage, time resolution, large dynamic range) and location (4300 m above sea level) allowed both lowering the energy threshold down to the region covered by direct measurements, and reaching the knee of the all-particle spectrum where data from many ground based experiment are available since long time. Moreover, the possibility of a detailed study of the particle distribution at ground in the first few meters from the shower axis, provided a new and efficient way of selecting events initiated from light mass primaries (i.e. protons and alpha particles), without relying on the muon signal, thus avoiding an important part of the systematic dependencies on the adopted hadronic interaction model. The resulting all-particle spectrum (measured in the energy range $80\text{TeV} \rightarrow 20\text{PeV}$) is in good agreement with both theoretical parametrizations and previous measurements, thus validating the selection and reconstruction procedures. The light-component (i.e. p + He) spectrum has been measured from 30 TeV up to 3 PeV. The result, while being consistent with highest energy direct measurements, shows a clear indication of a bending below 1 PeV. This is in agreement with other two independent analyses of ARGO-YBJ data (one of them also using the Cherenkov signal as measured by a LHAASO telescope prototype), and provides new important inputs to acceleration/propagation models for galactic cosmic rays.

*The 34th International Cosmic Ray Conference,
30 July- 6 August, 2015
The Hague, The Netherlands*

*Speaker.

1. Introduction

Since its first experimental evidence in 1958 [1] the energy region around the knee in the all-particle cosmic ray (hereafter CR) spectrum has been investigated by several experiments with different approaches [2]. Below the knee, recent measurements carried out by the balloon-borne CREAM experiment [3,4] show that the proton and helium spectra from 2.5 to 250 TeV are harder compared to lower energy measurements. As pointed out by several authors, the evolution of the proton and helium spectra and their subtle differences could be indications of the presence of different populations of CR sources contributing to the overall flux and operating in environments with different chemical compositions [5,6]. Diffusion effects during CR propagation in the Galaxy might also play an important role.

In the knee region (and above) the measurements of the CR primary spectrum are carried out by EAS arrays. In this case mass composition studies are extremely difficult and often affected by large systematic uncertainties. The average composition at the knee is considered to be dominated by light elements, and the knee itself is interpreted as the steepening of the p and He spectra [7]. However, several experimental results suggest a heavier composition at knee energies [8–13].

A measurement of the CR primary energy spectrum (all-particle and light-component) in the $10^{12} \rightarrow 10^{16}$ eV energy range is under way with the ARGO-YBJ experiment (for a description of the detector and a report on some physics results see [14]). In order to cover this very wide energy range, different approaches have been followed:

- '*Digital*' analysis. It is based on the RPC digital readout system (i.e. on the strip multiplicity), and is sensitive in the 3 TeV - 300 TeV range [15, 16].
- '*Analog*' analysis. It uses the information coming from the RPC analog readout, thus exploring the 30 TeV-20 PeV energy range. The energy is reconstructed on an event-by-event basis by measuring the particle densities (and their lateral distribution) close to the shower axis. It is the subject of the present paper.
- '*Analog-Bayes*' analysis. Same as above but the energy is reconstructed in a complete different way, on a statistical basis, by using a bayesian approach. The selection of light elements (i.e. p+He) is also different, even if based (as in the previous analysis) on the particle lateral distribution. It is fully discussed in [17].
- '*Hybrid*' analysis. It is carried out by combining the data coming from ARGO-YBJ and a wide field of view Cherenkov telescope, exploring the 100 TeV - 3 PeV region [18, 19].

The results concerning the all-particle and the light-component (i.e. p+He) spectra, so far obtained with the aforementioned '*Analog*' analysis, will be described in the following sections. A more comprehensive discussion on the reconstruction of EAS properties, as part of this analysis, is given in [20].

2. Event reconstruction and measurement of the all-particle spectrum

The RPC charge readout system of the ARGO-YBJ detector allows studying the structure of the particle density distribution in the shower core region up to particle densities of about $10^4/\text{m}^2$ [21, 22]. The study of the particle lateral density function (LDF) close to the shower axis is expected to provide information on its longitudinal profile in the atmosphere, that is to estimate its

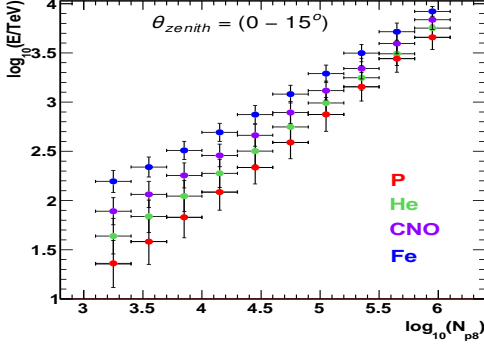


Figure 1: The primary energy as a function of the reconstructed truncated size N_{p8} (within 8 m from the axis) for simulated showers initiated by different primary nuclei.

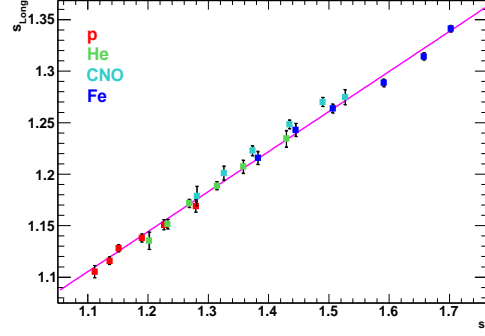


Figure 2: The longitudinal age parameter s_{long} vs the lateral age s' resulting from the fit of the reconstructed LDF, for simulated showers initiated by different primary nuclei (see text).

development stage, or the so-called *age*, which is related to X_{max} , the atmospheric depth at which the cascade reaches its maximum size. This implies the possibility of selecting showers within given intervals of X_{max} or, equivalently, of $X_{dm} \equiv X_{det} - X_{max}$, the grammage between the depth of the shower maximum and the detection level. For this reason, the combined use of the shower energy and age estimations can ensure a sensitivity to the primary mass, thus giving the possibility of selecting a light (p+He) event sample with high efficiency.

As fully discussed in [20], various observables were considered and analyzed in order to find a suitable estimator for the primary CR energy. Among them, according to MC simulations, N_{p8} , the number of particles detected at ground within a distance of 8 m from the shower axis, resulted well correlated with energy, not biased by the finite detector size and not much affected by shower to shower fluctuations. Nevertheless, as shown in Fig. 1, this truncated size is a mass-dependent energy estimator parameter. In order to have a mass-independent parameter we fitted the LDFs of individual showers (up to ten meters from the core) event-by-event, for different N_{p8} intervals and different shower initiating primaries, with a suitable function to get the shape parameter s' (see [20] for details).

From these studies we find that, for a given primary, the s' value decreases when N_{p8} (i.e. the energy) increases, this being due to the observation of younger (deeper) showers at larger energies. Moreover, for a given range of N_{p8} , s' increases going from proton to iron, as a consequence of older (shallower) showers. Both dependencies are in agreement with the expectations, the slope s' being correlated with the shower age, thus reflecting its development stage. This outcome has two important implications, since the measurements of s' and N_{p8} can both (i) help constraining the shower age and (ii) give information on the primary particle nature.

Concerning the first point, we show in Fig.2 the average value of the longitudinal shower age parameter $s_{long} \equiv 3X_{det}/(X_{det} + 2X_{max})$, for each simulated primary type and N_{p8} interval, as a function of the LDF slope parameter s' (i.e. the so-called *lateral age* [23]), as obtained from the fit of each reconstructed event. As can be seen, the shape parameter s' depends only on the development stage of the shower, independently from the nature of the primary particle. This expresses an important universality of the LDF of detected EAS in terms of the lateral shower

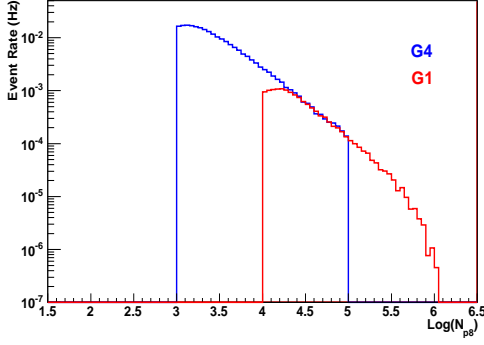


Figure 3: The N_{p8} distributions for the two real data samples with different gain setting configurations (see text).

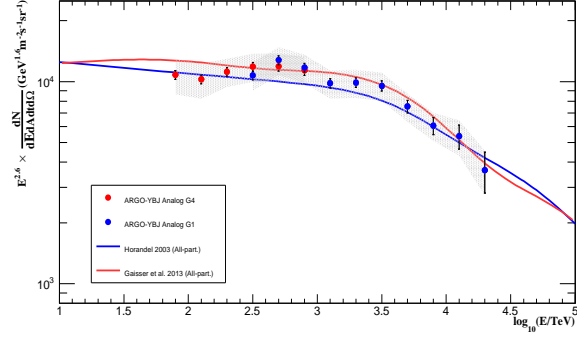


Figure 4: The all-particle energy spectrum of primary CRs resulting from this work. The parametrizations provided by [5] and [24] are shown for comparison.

age. The LDF slope s' is a mass-independent estimator of the average s_{long} (or X_{max}). Obviously shower-to-shower fluctuations introduce unavoidable systematics, whose effects can be anyway quantified and taken into account. Another implication is that s' from the LDF fit close to the shower axis, together with the measurement of the truncated size N_{p8} , can give information on the primary particle nature, thus making possible the study of mass composition and the selection of a light-component data sample (see below).

By assuming an exponential absorption after the shower maximum, we get N_{p8}^{max} , a variable linearly correlated to the size at the shower maximum, using N_{p8} and s' measurements for each event and simply correcting with: $N_{p8}^{max} \approx N_{p8} \cdot \exp[(h_0 \sec \theta - X_{max}(s'))/\lambda_{abs}]$. A suitable choice of the absorption length λ_{abs} ($=100 \text{ g/cm}^2$) allows to get N_{p8}^{max} , a parameter correlated with primary energy in an almost linear and mass independent way, providing an energy estimator with a $\text{Log}(E/\text{TeV})$ resolution of 0.10–0.15 (getting better with energy) and $\text{Log}(E/\text{TeV})$ bias less than 0.05 [20]. We also checked that using more realistic parametrizations of the EAS longitudinal absorption, given the age values and the role of shower-to-shower fluctuations, leads to consistent results

As described in [21], the RPC charge readout system has 8 different and overlapping gain scale settings (G0, ..., G7 from smaller to larger gains, with nominal shifts of a factor two) in order to explore the particle density range $\approx 20 - 10^4 \text{ particles/m}^2$. In this analysis the results obtained with two gain scales (so-called G1 and G4) are presented. The analog system response, for each considered data set and gain scale has been carefully calibrated by following the procedures fully discussed in [21, 22]. In Fig.3 the N_{p8} distributions are shown for two real data samples (with different gain setting configurations), in the intervals considered for this analysis. As can be seen, the overlap among different gain scales is more than satisfactory, thus also validating the adopted calibration procedure.

Selecting quasi-vertical events ($\theta < 15^\circ$) with different values of the truncated size N_{p8} , using the described procedure, we reconstructed the CR all-particle energy spectrum shown in the Fig.4 in the energy range $80 \text{ TeV} \rightarrow 20 \text{ PeV}$. In the plot the overall systematic uncertainty, due to hadronic interaction models, selection criteria, unfolding algorithms, and aperture calculation, is shown by

the shaded area. The statistical uncertainty is shown by the error bars. As can be seen from the figure, spectra obtained by analyzing two different data samples with two different gain settings, actually overlap. Moreover preliminary results of the analysis of a third independent data sample, and using the G0 gain scale, are in agreement within the quoted uncertainties. The resulting all-particle spectrum is in fair agreement with the parametrizations provided by [5] and [24], showing evidence of a change of the spectral index at an energy consistent with the position of the knee. As shown in Fig.7 this result is also consistent with previous measurements made by both direct and indirect experiments. This is also regarded as an important check on the absolute energy scale set for this analysis, whose systematic uncertainty has been anyhow conservatively estimated at the level of 10%, and is in agreement with another independent analysis of ARGO-YBJ data [25].

3. Measurement of the light-component energy spectrum

Starting from the initial data set used for the measurement of the all-particle spectrum, a selection has been made in order to have a sample of p and He initiated showers, with sufficiently high efficiency and low contamination. This has been possible on the basis of the simultaneous study of the LDF slope s' and the truncated size N_{p8} (see Sec.2 and [20]).

In Fig. 5 the values of s' are shown as a function of N_{p8} , as reconstructed for different samples of simulated data resulting from EAS initiated by protons, helium, CNO (i.e. Carbon-Nitrogen-Oxygen) group, and iron nuclei. As in the previous plots, the fluxes have been parametrized as in [24], and the full simulation of detector response and analysis procedures has been applied. A different parametrization of the single fluxes, namely [5], gives consistent results within the quoted systematics (see below). The line in the plots shows the cut used in selecting the p+He enriched sample from real data. The efficiency in selecting p and He initiated showers and the heavier elements contamination are at the level of 90% and 10% respectively, with variations of few percent depending on the energy region and the adopted flux parametrizations.

Taking into account these values (and their energy dependence), the p+He flux has been obtained. The result is shown in Fig.6. The systematic uncertainty on the flux is shown by the shaded area and the statistical one by the error bars. A systematic uncertainty on the energy scale at the level of 10% has also been conservatively estimated (not shown in the plots). Moreover we conservatively decided not to subtract the estimated contamination of heavier elements, adding their contribution in the systematic uncertainty on the flux. The parametrizations of the light-component provided by [5] and [24] are shown by the red and blue dashed lines, respectively. A modified version of the fluxes given in [24], with each knee at $Z \times 1$ PeV (i.e. about a factor four lower in energy than in the original formulation), is also shown for comparison. As can be seen also from Fig.7, the result is consistent with low energy (direct) measurements and show a clear evidence for a bending at larger energies but starting below 1 PeV. Also in this case, preliminary results of the same analysis applied to a third independent data sample and using the G0 gain scale are in agreement within the quoted uncertainties.

The evidence for the spectral bending is also given by a different analysis of ARGO-YBJ data (namely the 'Analog-Bayes' one) using a bayesian approach [17]. Moreover a third analysis (namely the 'Hybrid' one), that actually combines data coming from ARGO-YBJ and a wide field

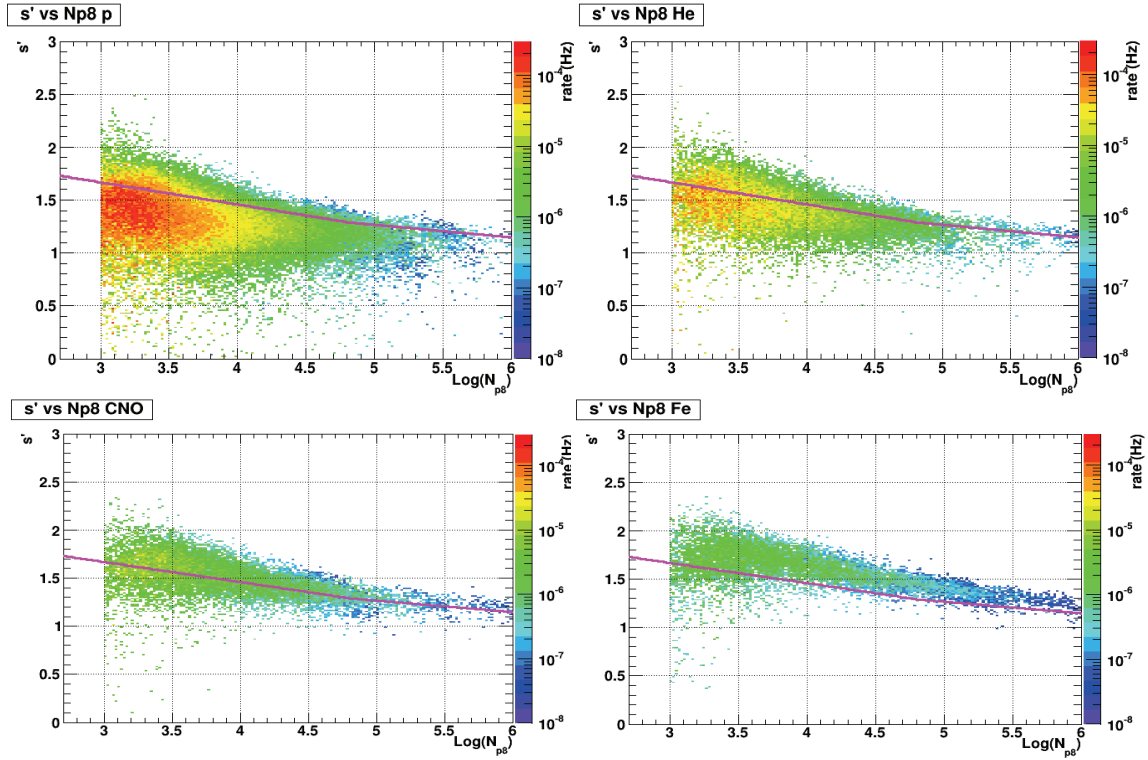


Figure 5: The LDF slope s' as a function of the truncated size N_{p8} as reconstructed for showers initiated by different primary nuclei, as indicated in the upper left labels. The p+He selection cut is shown by the pink line.

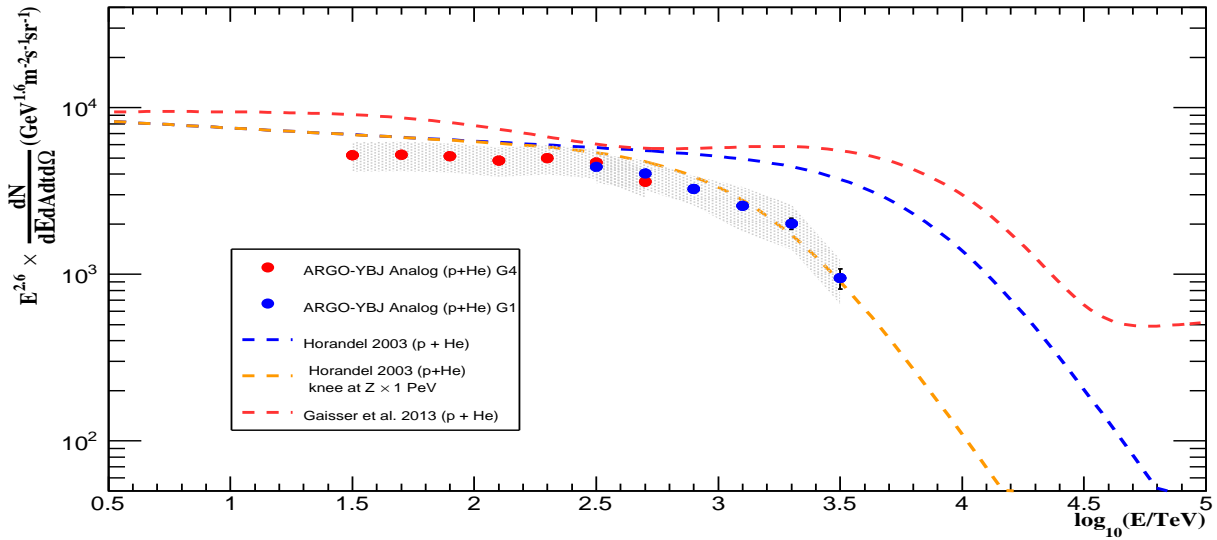


Figure 6: Light (i.e. p+He) component energy spectrum of primary CRs as measured in this work (see text).

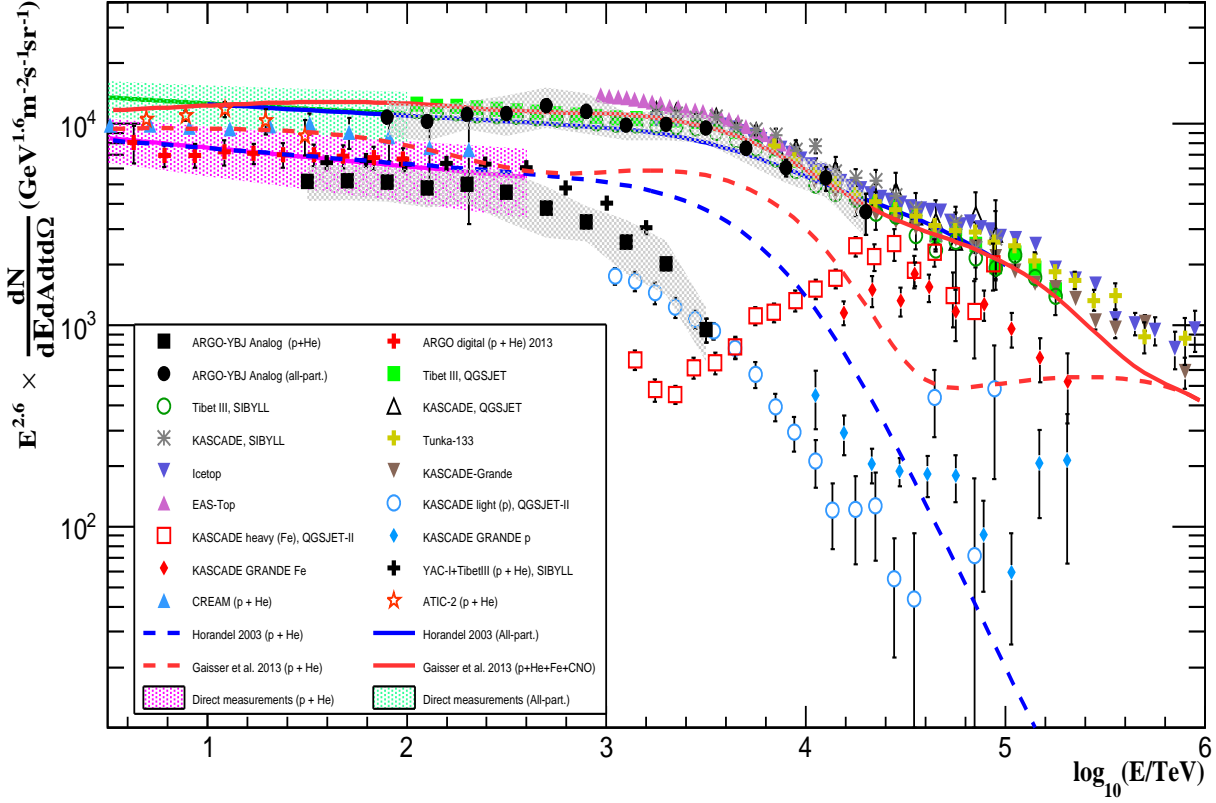


Figure 7: The all particle and light (p+He) component energy spectra of primary CRs as measured in this work, compared to several other experimental results [26].

of view Cherenkov telescope, also gives consistent results, within the systematic uncertainties and the possible difference in the energy scale [18, 19].

4. Conclusions

The results of an analysis technique, based on the study of the number of charged particles at ground and the shape of their lateral density distribution within the first ten meters from the shower axis, with the ARGO-YBJ detector, have been reported.

The cosmic ray all-particle spectrum has been measured in the 80 TeV-20 PeV energy region, by using two different data samples taken with two different gain settings of the RPC analog read-out system. Results are in agreement with previous observations from both direct and indirect experiments, thus validating the analysis strategy and the event reconstruction procedures.

A suitable selection of the light-component (i.e. protons and helium nuclei) has then been applied and its energy spectrum has been measured from 30 TeV up to 3 PeV. The result, while being consistent with highest energy direct measurements, shows a clear indication of a bending below 1 PeV. This is also consistent with other two independent analyses of ARGO-YBJ data

(one of them using in addition the information coming from a Cherenkov telescope). The study of possible improvements on event selection procedures and a complete analysis of systematic uncertainties is currently under way.

References

- [1] G.V. Kulikov and G.B. Khristiansen, *J. Exp. Theor. Phys.* 35 (1958) 635
- [2] J. Blümer, R. Engel, J.R. Hörandel, *Prog. Part. Nucl. Phys.* 63 (2009) 293 and references therein
- [3] H.S. Ahn et al., *Astrophys. J. Lett.* **714**, L89 (2010).
- [4] Y.S. Yoon et al., *Astrophys. J.* **728**, 122 (2011).
- [5] T.K. Gaisser, T. Stanev, S. Tilav, *Front. Phys.* 8(6) (2013) 748.
- [6] D. Caprioli et al., *Astrop. Phys.* **34**, 447 (2011).
- [7] W.D. Apel et al., *Astrop. Phys.* **31**, 86 (2009).
- [8] M. Aglietta et al., *Astrop. Phys.* **21**, 223 (2004).
- [9] M. Ambrosio et al. *Phys. Rev. D* 56 (1997) 1418
- [10] M. Amenomori et al., *Phys. Lett. B* **632**, 58 (2006).
- [11] H. Tokuno et al., *Astrop. Phys.* **29**, 453 (2008).
- [12] H. T. Freudenreich et al., *Phys. Rev. D* **41**, 2732 (1990).
- [13] M.A.K. Glasmacher et al., *Astrop. Phys.* **12**, 1 (1999).
- [14] I. De Mitri et al. (ARGO-YBJ coll.), *Nucl. Instr. and Meth. in Phys. Res.* A742 (2014) 2-9
- [15] B. Bartoli et al. (ARGO-YBJ coll.), *Phys. Rev. D* **85**, 092005 (2012).
- [16] B. Bartoli et al. (ARGO-YBJ coll.), arXiv:1503.07136 (2015)
- [17] P. Montini et al. (ARGO-YBJ coll.), in Proc. 34th ICRC, (The Hague, 2015) **ID: 961**
- [18] B. Bartoli et al. (ARGO-YBJ coll.), *Chinese Phys. C* **38**, 045001 (2014).
- [19] S. Zhang et al. (ARGO-YBJ coll.), in Proc. 34th ICRC, (The Hague, 2015) **ID: 315**
- [20] P. Bernardini et al. (ARGO-YBJ coll.), in Proc. 34th ICRC, (The Hague, 2015) **ID: 1029**
- [21] B. Bartoli et al. (ARGO-YBJ coll.), *Astrop. Phys.* 67 (2015) 47-61
- [22] B. Bartoli et al. (ARGO-YBJ coll.), *Nucl. Instr. and Meth. in Phys. Res.* A783 (2015) 68-75
- [23] R.K. Dey et al., in Proc. 32nd ICRC, (Beijing, 2011), vol.1, pag.174
- [24] J.H. Hörandel, *Astrop. Phys.* **19**, 193 (2003).
- [25] M. Iacovacci et al. (ARGO-YBJ coll.), in Proc. 34th ICRC, (The Hague, 2015) **ID: 993**
- [26] M. Amenomori et al., *Astrophys. J.* 678 (2008) 1165 – M. Amenomori et al., in Proc. 33rd ICRC, (Rio de Janeiro, 2013), paper ID:1047 – T. Antoni et al., *Astroparticle Physics* 24 (2005) 1-25 – W.D. Apel et al., *Astroparticle Physics* 36 (2012) 183-194 – S.F. Bereznev et al., *Nucl. Instr. and Meth. in Phys. Res.* A692 (2012) 98-105 – M. G. Aartsen et al., *Phys. Rev. D* 88, 042004 (2013) – M. Aglietta et al., *Astroparticle Physics* 10 (1999) 1-9 – D. Panov et al., *Bull. Russian Acad. Sci. Phys.* 73 (2009) 564-567 – Y.S. Yoon et al., *Astrophys. J.* 728, (2011) 122